Published by Institute of Physics Publishing for SISSA/ISAS
Received: December 2, 2003
Accepted: December 4, 2003

Theoretical uncertainties on α_s from event-shape variables in e^+e^- annihilations

Roger W. L. Jones
Lancaster University, Lancaster, LA1 4Yb, U.K.
Email: Roger.Jones@cern.ch

Matthew Ford
Cavendish Laboratory, Madingley Road, Cambridge, CB3 0HE, U.K.
Email: Matthew.Ford@cern.ch

Gavin P. Salam
LPTHE, Universités Paris VI and VII, and CNRS UMR 7589
Paris 75005, France
Email: salam@lpthe.jussieu.fr

Hasko Stenzel
II. Physikalisches Institut, JLU Giessen
Heinrich-Buff Ring 16, D-35392 Giessen, Germany
Email: Hasko.Stenzel@exp2.physik.uni-giessen.de

Daniel Wicke
Bergische Universität, Gaußstr. 20, D-42097 Wuppertal, Germany
Email: Daniel.Wicke@physik.uni-wuppertal.de

Abstract: The precision of measurements of the strong coupling constant using event-shape variables in e^+e^- annihilations is limited by theoretical systematic uncertainties. The uncertainties are related to missing higher orders in the perturbative predictions for the event-shape distributions. A new method is presented for the assessment of theoretical uncertainties in α_s. This method evaluates the systematic uncertainty of the parameter α_s from the uncertainty of the prediction for the distributions from which it is extracted. The perturbative uncertainties are calculated on a purely theoretical basis, without accessing measured distributions. The method is therefore especially suited for an unbiased combination of results from different observables or experiments.
It is universal and can be applied to other processes like jet production in deep-inelastic *ep* scattering or in hadron collisions.

Keywords: QCD, NLO Computations, Jets.

Contents

1. Introduction

Studies of Quantum Chromodynamics in e^+e^- annihilations have been carried out over more than 30 years at increasing centre-of-mass energies. Event-shape variables have proven to be key observables in both annihilation and deep-inelastic scattering processes. The understanding of perturbative and non-perturbative aspects of QCD has grown with the study of event shapes. While event shapes were first introduced to characterise global properties, it was soon realised that their distributions are sensitive to the strong coupling constant α_s. The perturbative prediction for a generic infrared-collinear (IRC) safe event-shape variable y can be computed to second order in α_s,

$$\frac{1}{\sigma}\frac{d\sigma}{dy} = A(y)\frac{\alpha_s}{2\pi} + B(y)\left(\frac{\alpha_s}{2\pi}\right)^2, \tag{1.1}$$

with coefficient functions A and B obtained from integration of the ERT [1] matrix elements. Using this type of prediction, first determinations of α_s were performed at the PEP and PETRA colliders. In the era of the LEP experiments the calculations for certain classes of variables were improved by resumming leading and next-to-leading logarithmic terms (NLL). These calculations, matched to fixed-order expressions, enlarged the kinematic range of applicability for α_s extractions and reduced the systematic theoretical uncertainty. Recently, event-shape variables have also been used extensively to study non-perturbative power law corrections. It has been shown that hadronisation corrections, scaling with inverse powers of the momentum transfer Q can be modelled with one or a few non-perturbative parameters [2]. These parameters can in turn be related to moments of an effective coupling at low scales, and have been extracted from the data [3].

JHEP12(2003)007

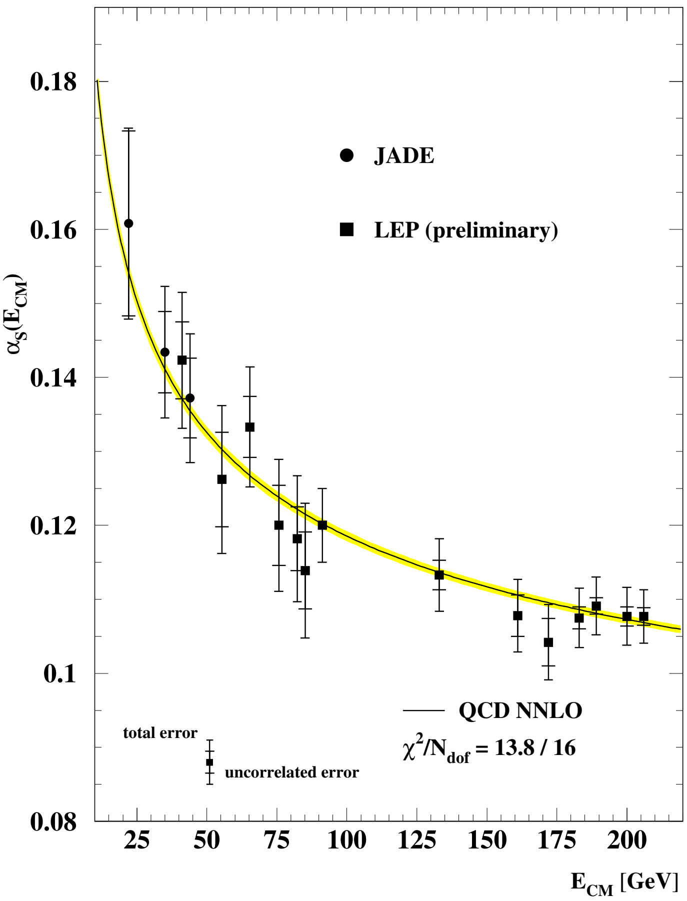

Figure 1: Measurements of α_s from event-shape variables as function of centre-of-mass energy.

At present measurements of α_s using event-shape variables and $\mathcal{O}(\alpha_s^2)$+NLL resummed calculations are available at centre-of-mass energies between 22 GeV and 206 GeV. For illustration a selection of these measurements is shown in figure 1.

New measurements re-analysing data from the JADE collaboration [4] were performed using a technique similar to that applied for a combined analysis by the LEP collaborations [5]. In particular, the same theoretical framework was used and at most of the energies a similar set of variables was combined. At almost all energies perturbative theoretical uncertainties dominate other systematic uncertainties, e.g. at $Q = M_Z$ the perturbative uncertainty is 5% and the quadratic sum of statistical, experimental and hadronisation uncertainties is 1.3%.

It is the objective of this note to examine ways of estimating the theoretical uncertainties and to propose a comprehensive and consistent method to combine different uncertainty estimates. In addition, the proposed method should allow the calculation of the uncertainty associated with a given measurement without using the data from which α_s is extracted. This is notably important for global combinations of various measurements, where a coherent procedure must be applied.

The origin of perturbative theoretical uncertainties is the truncation of the perturbative series at a given order of the coupling constant, whereby the truncated prediction acquires a dependence on the renormalisation scale.

To illustrate this point, a fully inclusive observable, the total hadronic cross section $\sigma(\mathrm{e^+e^-} \to \mathrm{q\bar{q}})$, is considered as an example for which third order $\mathcal{O}(\alpha_s^3)$ calculations are available. The ratio R_Z of hadronic to leptonic widths at the Z boson resonance reads (with renormalisation scale $\mu = Q$) [6]

$$R_\mathrm{Z} = \frac{\Gamma(\mathrm{Z}^0 \to \mathrm{hadrons})}{\Gamma(\mathrm{Z}^0 \to \mathrm{leptons})} = R_\mathrm{EW} \sum_{n=0}^{3} c_n \left(\frac{\alpha_s}{\pi}\right)^n \tag{1.2}$$

with

$$R_\mathrm{EW} = 19.934\,, \qquad c_0 = 1\,, \qquad c_1 = 1.045\,, \qquad c_2 = 0.94\,, \qquad c_3 = -15\,. \tag{1.3}$$

One estimate of the theoretical uncertainty on R_Z is based on the size of the last term in the series, taking the difference between the full next-to-next-to-leading order (NNLO) prediction and the next-to-leading order (NLO) truncation. Taking the preliminary combined LEP measurement $R_\mathrm{Z} = 20.767 \pm 0.025$ [7] the NNLO result is $\alpha_s(M_\mathrm{Z}) = 0.1240 \pm 0.0037(exp)$ and the central value shifts down to $\alpha_s^{NLO}(M_\mathrm{Z}) = 0.1214$ when the NLO prediction is used. Hence, the theoretical uncertainty estimated by the NNLO to NLO difference is $\Delta\alpha_s = \pm 0.0026$. The 'true' error would be the difference between the NNLO result and the complete theory. The NNLO to NLO difference can only be a good estimate of that if the convergence of the perturbation series is fast enough, i.e. if the size of the expansion coefficients remains of order unity. In the case of R_Z, however, the size of the third order term amounts to 60 % of the second order term size.

Of course the size of the last known term of the series is not the only way of estimating the uncertainty on the prediction. Another method originates from the fact that dimensional regularisation, used to define formally divergent loop corrections prior to $\overline{\mathrm{MS}}$ renormalisation, requires the introduction of a renormalisation scale μ at which the coupling, $\alpha_s(\mu^2)$, is defined. While the choice of scale is arbitrary, higher-order perturbative corrections contain terms proportional to powers of $\ln \mu^2/Q^2$, which order-by-order compensate for the scale dependence of the coupling. Only in the presence of all orders this compensation is complete. For a calculation to order α_s^n there is residual scale-dependence of order α_s^{n+1}; since it would be cancelled by higher order terms, its size can be taken as indicative of the magnitude of missing higher-order contributions.

The scale dependence of eq. (1.2) is given by the dependence of the NLO and NNLO coefficients on the scale parameter $x_\mu = \mu/Q$ as follows

$$c_2(x_\mu) = c_2^0 + \beta_0 c_1 \ln x_\mu^2 \tag{1.4}$$

$$c_3(x_\mu) = c_3^0 - \left(2\beta_0 c_2^0 + c_1\beta_1\right) \ln x_\mu^2 + c_1 \beta_0^2 \ln^2 x_\mu^2\,, \tag{1.5}$$

where the coefficients c_i^0 are those of eq. (1.3) and the first three coefficients of the β function are

$$\beta_0 = \frac{33 - 2n_f}{12}\,, \qquad \beta_1 = \frac{153 - 19n_f}{24}\,, \qquad \beta_2 = \frac{1}{64}\left[\frac{2857}{2} - \frac{5033}{18} n_f + \frac{325}{54} n_f^2\right]. \tag{1.6}$$

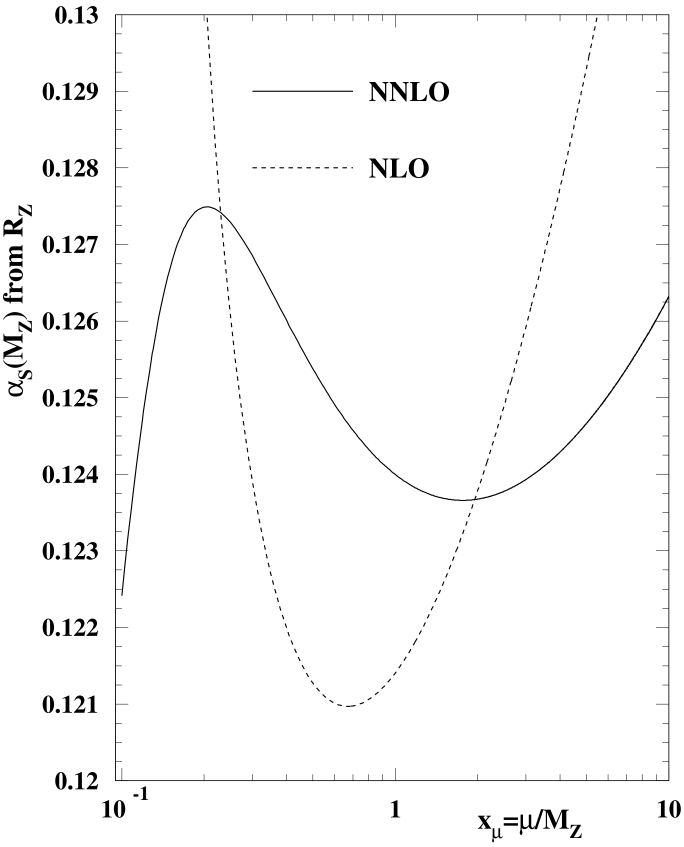

Figure 2: The dependence on the renormalisation scale parameter of $\alpha_s(M_Z)$ using R_Z at NNLO (solid line) and at NLO (dashed line).

The number of active flavours n_f is taken to be five at $Q = M_Z$. The renormalisation scale dependence of the coupling constant can be parameterised in the modified minimal subtraction scheme at 3-loop level [8] as a function of the scale $\Lambda \equiv \Lambda_{\overline{\rm MS}}^{(nf)}$

$$\alpha_s(\mu) = \frac{\pi}{\beta_0 \ln(\mu^2/\Lambda^2)} \left[1 - \frac{\beta_1}{\beta_0^2} \frac{\ln\left[\ln(\mu^2/\Lambda^2)\right]}{\ln(\mu^2/\Lambda^2)} + \frac{1}{\beta_0^2 \ln^2(\mu^2/\Lambda^2)} \times \right.$$
$$\left. \times \left(\frac{\beta_1^2}{\beta_0^2} \left\{ \ln^2\left(\frac{\mu^2}{\Lambda^2}\right) - \ln\left[\ln\left(\frac{\mu^2}{\Lambda^2}\right)\right] - 1 \right\} + \frac{\beta_2}{\beta_0} \right) \right]. \qquad (1.7)$$

The dependence of the measurement of $\alpha_s(M_Z)$ using R_Z is illustrated in figure 2. The case of R_Z nicely demonstrates the evolution of the scale dependence from NLO to NNLO. The structure of the perturbative series indicates that a natural value for the scale μ is of order M_Z, but its exact value is undetermined.

In e^+e^- annihilation it has become customary to take a central value of $x_\mu = 1$ and to estimate an uncertainty in the prediction by varying x_μ between 1/2 and 2. (In contrast, in global analyses of parton distribution functions it is sometimes x_μ^2 that is varied in that range, e.g. [9].) A variation of x_μ from 1/2 to 2 applied to R_Z yields a theoretical uncertainty for α_s of ± 0.0020, slightly lower than, but of the same general size as that obtained from the NNLO to NLO difference. This is despite the fact that the uncertainty from the x_μ variation is formally higher order in α_s than that from the NNLO to NLO difference.

In contrast to R_Z, event-shape distributions, which shall be studied in this paper, are known only to next-to-leading accuracy. In principle here too the last term of the series could be used to estimate the uncertainty. However, this is often seen as unduly conservative (it would give an uncertainty of order α_s^2, whereas missing terms are of order α_s^3) and the standard approach for NLO fixed-order calculations is to use just scale variations to estimate uncertainties.

Also in contrast to the R_Z case, over a significant part of the phase-space the event-shape distributions have *divergent* (or very poorly convergent) perturbative expansions, due to logarithmic enhancements of the perturbative coefficients. As a result, it is necessary to supplement fixed-order results with resummed calculations [10]–[15], leading to a series with two expansion parameters — the coupling and the logarithm of the observable. Estimating uncertainties on the result is considerably more involved than for a traditional fixed-order expansion. For example, in the same way that the presence of a formally arbitrary scale x_μ for the coupling is associated with an uncertainty, a new formally arbitrary scale x_L appears in the definition of the logarithm and it too is associated with an uncertainty on the perturbative prediction. Further uncertainties arise from freedom in the way resummed and fixed-order predictions are combined ('matched').

A number of these possible sources of uncertainty have come to light only recently, partly in the context of DIS event-shape resummations [16]. There is therefore a need for a comprehensive up to date study of the whole range of such uncertainties for e^+e^- event shapes, as well as an understanding of how to combine them. That is the purpose of the present article.

The definitions of the event-shape variables are given in section 2, in section 3 the theoretical predictions are summarised, in section 4 the methods for estimating and combining theoretical uncertainties are presented, in section 5 results obtained with the new method are discussed and the recommendation for an uncertainty strategy is summarised in section 6.

2. Definition of the event-shape variables

Event-shape variables are infrared and collinear safe observables that characterise global properties of hadronic events. They are experimentally measured with the momenta of charged and/or neutral particles. The variables are normalised so as to be dimensionless and independent of the production cross-section. One end of the spectrum is given by the two-jet limit, the other by a kinematic limit $y_{\max}$, which in some cases corresponds to either spherical or symmetric event configurations. The following variables are studied here.

Thrust T [17]: the thrust axis unit vector $\vec{n}_T$ maximises the following quantity:

$$T = \max_{\vec{n}_T}\left(\frac{\sum_i |\vec{p}_i \cdot \vec{n}_T|}{\sum_i |\vec{p}_i|}\right), \quad \tau = 1 - T\,, \tag{2.1}$$

where the thrust sum extends over all particles i in the event. It is convenient to define $\tau = 1 - T$ for the resummed expressions.

Heavy jet mass ρ [18]: a plane perpendicular to $\vec{n}_T$ divides the event into two hemispheres, H_1 and H_2, from which one obtains the corresponding normalised hemisphere (squared) invariant masses:

$$M_i^2 = \left(\sum_{k \in H_i} p_k \right)^2 , \quad i = 1, 2 . \tag{2.2}$$

The larger of the two hemisphere masses is called the heavy jet mass:

$$\rho \equiv M_H^2 = \frac{1}{E_{vis}^2} \max(M_1^2, M_2^2) , \tag{2.3}$$

where E_{vis} is the total visible energy in the event.

Wide jet broadening B_W [19]: a measure of the broadening of particles in transverse momentum with respect to the thrust axis can be calculated for each hemisphere H_i using the relation:

$$B_i = \frac{\sum_{k \in H_i} |\vec{p}_k \times \vec{n}_T|}{2 \sum_j |\vec{p}_j|}, \quad i = 1, 2 , \tag{2.4}$$

where j runs over all of the particles in the event. The wide jet broadening is the larger of the two hemisphere broadenings:

$$B_W = \max(B_1, B_2) . \tag{2.5}$$

Equivalently, the narrow jet broadening $\boldsymbol{B_N}$ is defined as $B_N = \min(B_1, B_2)$.

Total jet broadening B_T: the total jet broadening is the sum of the wide jet broadening and the narrow jet broadening:

$$B_T = B_W + B_N . \tag{2.6}$$

C-parameter C [20]: the C-parameter is derived from the eigenvalues of the linearised momentum tensor $\Theta^{\alpha\beta}$:

$$\Theta^{\alpha\beta} = \frac{1}{\sum_i |\vec{p}_i|} \sum_i \frac{p_i^\alpha p_i^\beta}{|\vec{p}_i|} , \quad \alpha, \beta = 1, 2, 3 . \tag{2.7}$$

The three eigenvalues λ_j of this tensor define C with:

$$C = 3 \cdot (\lambda_1 \lambda_2 + \lambda_2 \lambda_3 + \lambda_3 \lambda_1) . \tag{2.8}$$

Durham jet resolution parameter y_3 [21]: the Durham clustering algorithm for jet rates is taken as follows. For each pair of particles i and j in an event the metric y_{ij} is computed:

$$y_{ij} = \frac{2 \min(E_i^2, E_j^2)(1 - \cos\theta_{ij})}{E_{vis}^2} (\text{Durham algorithm}) . \tag{2.9}$$

The pair of particles with the smallest value of y_{ij} is replaced by a cluster. The four-momentum of the cluster is taken to be the sum of the four momenta of particles i and j, $p^\mu = p_i^\mu + p_j^\mu$ ('E' recombination scheme). The clustering procedure is repeated until all y_{ij} values exceed a given threshold $y_{\rm cut}$. The number of clusters remaining at this point is defined to be the number of jets.

The $y_3 \equiv y_{23}$ jet resolution parameter is the threshold value of $y_{\rm cut}$ below which an event is classified as having two jets and above which it has three jets. The distribution of y_3 falls steeply, with only a very narrow peak at small y_3. In order to better examine the region of small y_3, the logarithmic form $-\ln y_3$ is usually analysed.

3. Theoretical predictions

In this section the ingredients of the theoretical calculations as well as methods for gauging the uncertainties are outlined. At the end of the section directions in which there is partial theoretical progress in improving the accuracies of the theoretical calculations are mentioned.

3.1 Theoretical ingredients

Fixed order calculation. To second order in α_s, the distribution of a generic event-shape variable y ($y{=}\tau$, ρ, B_T, B_W, C or y_3) is given by:

$$\frac{1}{\sigma_{\rm tot}}\frac{d\sigma(y)}{dy} = \overline{\alpha}_s(\mu^2)A(y) + \left(\overline{\alpha}_s(\mu^2)\right)^2\left[A(y)\,2\beta_0\ln x_\mu^2 + B(y)\right], \tag{3.1}$$

where

$$\overline{\alpha}_s = \frac{\alpha_s}{2\pi}, \qquad x_\mu = \frac{\mu}{Q}, \qquad \mu = \text{renormalisation scale}. \tag{3.2}$$

The coefficient functions A and B are obtained from integration of the ERT matrix elements, using for instance the integration program EVENT2 [22]. Consider the cumulative cross section:

$$R(y,\alpha_s) \equiv \frac{1}{\sigma_{\rm tot}}\int_0^y \frac{d\sigma(x,\alpha_s)}{dx}dx\,, \tag{3.3}$$

which may be cast into the second-order form

$$R^{\mathcal{O}(\alpha_s^2)}(y,\alpha_s) = 1 + \mathcal{A}(y)\overline{\alpha}_s + \left[\mathcal{A}(y)\,2\beta_0\ln x_\mu^2 + \mathcal{B}(y)\right]\overline{\alpha}_s{}^2\,, \tag{3.4}$$

where $\mathcal{A}$ and $\mathcal{B}$ are integrated forms of A and B, and the explicit scale dependence of α_s has been dropped for clarity.

Resummed calculations. For small values of y, the fixed-order expansion, eq. (3.1) fails to converge, because the fixed-order coefficients are enhanced by powers of $\ln 1/y$, $\mathcal{A}(y) \sim \ln^2 y$, $\mathcal{B}(y) \sim \ln^4 y$. To obtain reliable predictions in the region of $y \ll 1$ it is necessary to *resum* entire sets of logarithmic terms at all orders in α_s. Certain event shapes and jet rates have the property that double logarithms exponentiate allowing one to write

$$R(y,\alpha_s) = (1 + C_1\overline{\alpha}_s + C_2\overline{\alpha}_s + \ldots)\,e^{Lg_1(\alpha_s L)+g_2(\alpha_s L)+\alpha_s g_3(\alpha_s L)+\cdots} + \mathcal{O}(\alpha_s y)\,, \tag{3.5}$$

	T	ρ	C	B_W	B_T	$-\ln y_3$
C_1	1.053	1.053	5.44	1.826	1.826	−6.685
C_2	34	40	76.5	116.3	92	18.2
G_{11}	4	4	4	8	8	4
G_{12}	−2.67	−2.67	−2.67	−5.33	−5.33	−4/3
G_{21}	22	36	63.4	73.8	78.5	−7.2
G_{22}	−24.94	−13.24	−24.94	−15.09	−61.88	0.868
G_{23}	−10.22	−10.22	−10.22	−27.26	−27.26	−3.407

Table 1: Numerical values of the resummation coefficients, to $\mathcal{O}(\alpha_s^2)$ for $n_f = 5$.

where $L = \ln y_0/y$, with $y_0 = 1$ for $y = \tau$, ρ, y_3, B_T, B_W and $y_0 = 6$ for C-parameter. The function $g_1(\alpha_s L)$ resums leading logarithms (LL), while $g_2(\alpha_s L)$ resums next-to-leading logarithms (NLL), etc. Such a resummation scheme allows to make reliable predictions down to the region $\alpha_s L \sim 1$.[1] The $g_n(\alpha_s L)$ functions have expansions

$$g_n(\alpha_s L) = \sum_{i=1}^{\infty} G_{i,i+2-n} \overline{\alpha}_s{}^i L^{i+2-n} \,. \tag{3.6}$$

Expressions for the LL and NLL functions g_1 and g_2 have been derived for a range of observables [10]–[15]. Additionally the C_1 coefficients are known analytically, and the further subleading terms G_{21} and C_2 are known numerically [10]–[23]. Thus the current state of knowledge for resummed results can be written

$$R_{NLL}(y, \alpha_s) = \left(1 + C_1 \overline{\alpha}_s + C_2 \overline{\alpha}_s{}^2\right) \exp(L g_1(\overline{\alpha}_s L) + g_2(\overline{\alpha}_s L) + G_{21} L \overline{\alpha}_s{}^2) \,. \tag{3.7}$$

The full set of coefficients to $\mathcal{O}(\alpha_s^2)$ is given in table 1.

Matching fixed order to resummed calculations. Pure fixed-order expansions are valid from moderate y to large y ($\alpha_s \ln^2 y \ll 1$), while resummed calculations apply to small y ($y \ll 1$). To obtain predictions over the whole kinematical range it is necessary to *match* the two calculations. This involves adding the two calculations and subtracting off double counting. This alone is not sufficient because even after the subtraction of double counting, there remain terms from the $\mathcal{O}(\alpha_s^2)$ contribution, in particular a piece $G_{21} \bar{\alpha}_{\mathrm{s}}^2 L$, which would cause the matched event-shape distributions to have a $G_{21} \bar{\alpha}_{\mathrm{s}}^2/y$ divergence at small y. In contrast, the physical requirement is that the distribution should vanish at least as fast as a positive power of y. The matching procedure is therefore more involved than a simple subtraction of double-counting terms between the resummed and fixed-order contributions; the details are given below.

[1] It is to be noted that two different logarithmic classifications schemes are in use in the literature. The convention adopted here classifies the logarithms in $\ln R$ and stems from [11]. In certain other contexts (e.g. [21]) it is logarithms in R itself that are classified, so that LL means terms $\alpha_s^n L^{2n}$ in R, NLL gives terms $\alpha_s^n L^{2n-1}$, etc. Such a resummation scheme is valid in a more restricted range of L, $\alpha_s L^2 \lesssim 1$.

Matching can be performed either for R or the logarithm of R, the resulting expressions are identical to $\mathcal{O}(\alpha_s^2)$, but differ in the treatment of subleading terms. The prediction of the **Log(R)** matching scheme is given by [11]:

$$\begin{aligned}\ln R(y,\alpha_s) &= Lg_1(\alpha_s L) + g_2(\alpha_s L) - (G_{11}L + G_{12}L^2)\overline{\alpha}_s - \\ &\quad -(G_{22}L^2 + G_{23}L^3)\overline{\alpha}_s{}^2 + \mathcal{A}(y)\overline{\alpha}_s + \left[\mathcal{B}(y) - \frac{1}{2}\mathcal{A}^2(y)\right]\overline{\alpha}_s{}^2 \,.\end{aligned} \tag{3.8}$$

As the entire $\mathcal{O}(\alpha_s^2)$ term, $\mathcal{B}(y)$, is exponentiated by this procedure, the problem of unphysical divergence from the G_{21} term is avoided.

The expression for the **R** matching scheme reads [11]

$$\begin{aligned}R(y,\alpha_s) &= (1 + C_1\overline{\alpha}_s + C_2\overline{\alpha}_s{}^2)\exp\left[Lg_1(\alpha_s L) + g_2(\alpha_s L) + G_{21}L\overline{\alpha}_s{}^2\right] - \\ &\quad -G_{21}L\overline{\alpha}_s{}^2 - \left[C_1 + G_{11}L + G_{12}L^2\right]\overline{\alpha}_s - \\ &\quad -\left[C_2 + C_1(G_{11}L + G_{12}L^2) + \frac{1}{2}(G_{11}L + G_{12}L^2)^2 + (G_{22}L^2 + G_{23}L^3)\right]\overline{\alpha}_s{}^2 + \\ &\quad +\mathcal{A}(y)\overline{\alpha}_s + \mathcal{B}(y)\overline{\alpha}_s{}^2 \,.\end{aligned} \tag{3.9}$$

Here the G_{21} term is explicitly placed in the exponent, with the non-exponentiated fixed-order remainder vanishing as y is taken to zero.

The Log(R) scheme is generally preferred over the R scheme, because the latter requires explicit knowledge of G_{21} and C_2, which have to be evaluated numerically. The Log(R) expression is furthermore much simpler and it is believed to be theoretically more stable. This can be seen in the region of small y, where the remainder terms of the R scheme are found to be larger than the corresponding Log(R) terms.

3.2 Sources of arbitrariness

Modified matching. The predictions obtained with the Log(R) and R matching schemes suffer from a limitation: unlike fixed-order predictions, they do not vanish at the multi-jet kinematic limit. The $\mathcal{O}(\alpha_s^2)$ expressions vanish at the phase space limit for four-parton production. The matching schemes can be modified to overcome this drawback. To do this, a kinematic constraint is imposed to guarantee that the prediction of the distribution vanishes at a given value $y_{\max}$. This means for the **modified Log(R)** [11]

$$\ln R(y_{\max}) = 0\,,\ \frac{1}{\sigma_{\rm tot}}\frac{d\sigma(y)}{dy}\bigg|_{y=y_{\max}} = \frac{dR}{dy}\bigg|_{y=y_{\max}} = 0\,. \tag{3.10}$$

To fulfil this constraint L is replaced by

$$\tilde{L} = \frac{1}{p}\ln\left(\left(\frac{y_0}{y}\right)^p - \left(\frac{y_0}{y_{\max}}\right)^p + 1\right). \tag{3.11}$$

The power p is called the degree of modification and is usually chosen equal to unity. It determines how fast the distribution is damped at the kinematic limit. The nominal values of $y_{\max}$ are obtained for thrust, C-parameter and y_3 on the basis of symmetry arguments. For the other variables matrix element calculations were carried out and compared to

variable	τ	ρ	$-\ln y_3^*$	B_T	B_W	C	comment
$y_{\max}$	0.5	—	$\ln 3$	—	—	1	theoretical maximum
$y_{\max}$	0.4225	0.4175	1.100	0.4075	0.325	1	ME 4-partons
$y_{\max}$	0.428	0.394	1.102	0.397	0.307	0.994	PS partons
$y_{\max}$	0.434	0.383	1.103	0.396	0.295	0.995	PS hadrons
$y_{\max}$	0.5	0.42	$\ln 3$	0.41	0.33	1	nominal value
$y'_{\max}$	0.42	0.38	$\ln 3$	0.39	0.29	0.99	alternate lower value

Table 2: Values of $y_{\max}$ at which the distributions vanish. The 'ME 4-partons' entries have been determined from binned distributions and their accuracy is therefore limited by the resolution of the binning. *In the case of $-\ln y_3$ it is the minimal value, corresponding to $y_{3,max} = 1/3$.

various parton shower simulations using PYTHIA [24], the results of which are given in table 2. Ten million events were generated for the Monte Carlo simulation. Since the aim behind the modified matching formulae is to extend the distribution up to the true kinematic maximum of the observable, the maximum of all $y_{\max}$ determinations is taken as nominal $y_{\max}$ value. However, insofar as the prescription for this extension is quite arbitrary, for studies of the theoretical uncertainties it will also be instructive to examine, as an alternative for each observable, the lowest of the $y_{\max}$ values found in table 2 (see section 4).

While for the modification of Log(R)-matching the replacement of L with $\tilde{L}$ in eq. (3.8) is sufficient to fulfil the constraints of eq. (3.10) this is not true for the R-matching. To modify the R-matching in addition, the matching coefficients G_{11} and G_{12} become functions of y such that:

$$\tilde{L}(y_{\max}) = 0\,, \qquad \tilde{G}_{11}(y_{\max}) = 0\,, \qquad \tilde{G}_{21}(y_{\max}) = 0\,. \tag{3.12}$$

This is achieved with the following modification:

$$\begin{aligned}
\tilde{L}(y) &= \frac{1}{p}\ln\left[\left(\frac{y_0}{y}\right)^p - \left(\frac{y_0}{y_{\max}}\right)^p + 1\right], \\
\tilde{G}_{11}(y) &= G_{11}\left[1 - \left(\frac{y}{y_{\max}}\right)^p\right], \\
\tilde{G}_{21}(y) &= G_{21}\left[1 - \left(\frac{y}{y_{\max}}\right)^p\right].
\end{aligned} \tag{3.13}$$

Finally the expression for the **modified R** matching scheme can be written as

$$\begin{aligned}
\tilde{R}(y,\alpha_s) = {} & (1 + C_1\overline{\alpha}_s + C_2\overline{\alpha}_s{}^2) \times \\
& \times \exp\left[\tilde{L}g_1(\alpha_s\tilde{L}) + g_2(\alpha_s\tilde{L}) - \left(\frac{y}{y_{\max}}\right)^p G_{11}\overline{\alpha}_s\tilde{L} + \tilde{G}_{21}\tilde{L}\overline{\alpha}_s{}^2\right] - \\
& - \tilde{G}_{21}\tilde{L}\overline{\alpha}_s{}^2 - \left[C_1 + \tilde{G}_{11}\tilde{L} + G_{12}\tilde{L}^2\right]\overline{\alpha}_s - \\
& - \left[C_2 + C_1(\tilde{G}_{11}\tilde{L} + G_{12}\tilde{L}^2) + \frac{1}{2}(\tilde{G}_{11}\tilde{L} + G_{12}\tilde{L}^2)^2 + (G_{22}\tilde{L}^2 + G_{23}\tilde{L}^3)\right]\overline{\alpha}_s{}^2 + \\
& + \mathcal{A}(y)\overline{\alpha}_s + \mathcal{B}(y)\overline{\alpha}_s{}^2\,.
\end{aligned} \tag{3.14}$$

JHEP12(2003)007

Renormalisation scale dependence. For scale parameters x_μ different from unity, every second order terms acquires a scale dependence explicitly given by

$$\begin{aligned}
\mathcal{B}(y) \to \overline{\mathcal{B}}(y) &= \mathcal{B}(y) + 2\beta_0\,\mathcal{A}(y)\ln x_\mu^2\,, \\
G_{21} \to \overline{G}_{21} &= G_{21} + 2\beta_0\,G_{11}\ln x_\mu^2\,, \\
G_{22} \to \overline{G}_{22} &= G_{22} + 2\beta_0\,G_{12}\ln x_\mu^2\,, \\
C_2 \to \overline{C}_2 &= C_2 + 2\beta_0\,C_1\ln x_\mu^2\,, \\
g_2(\alpha_s L) \to \overline{g}_2(\alpha_s L) &= g_2(\alpha_s L) + \frac{\beta_0}{\pi}\,(\alpha_s L)^2\ g_1'(\alpha_s L)\ln x_\mu^2\,.
\end{aligned} \tag{3.15}$$

The overlined terms of eq. (3.15) replace for $x_\mu \neq 1$ the corresponding terms in equations (3.8) and (3.9). Of course the coupling constant itself exhibits the scale dependence indicated in eq. (1.7).

Rescaling resummed logarithms. In addition to the arbitrariness in the choice of μ there is also arbitrariness in the definition of the logarithms to be resummed; for example, whether powers of $\alpha_s \ln\frac{y_0}{y}$ or of $\alpha_s \ln\frac{2y_0}{y}$ are resummed. This can be formalised [16] by the introduction of an x_L parameter, analogous to x_μ, such that where normally powers of $\alpha_s \ln\frac{y_0}{y}$ are resummed instead, powers of $\alpha_s \ln\frac{y_0}{x_L y}$ are resummed. Such a rescaling alters the resummed formulae in the modified case according to:

$$\tilde{L} \to \widehat{L} = \frac{1}{p}\ln\left[\left(\frac{y_0}{x_L\cdot y}\right)^p - \left(\frac{y_0}{x_L\cdot y_{\max}}\right)^p + 1\right], \tag{3.16}$$

$$g_1(\alpha_s L) \to \widehat{g}_1 = g_1(\alpha_s \widehat{L})\,, \tag{3.17}$$

$$g_2(\alpha_s L) \to \widehat{g}_2 = g_2(\alpha_s \widehat{L}) + \ln x_L \frac{d}{d\widehat{L}}\left(\widehat{L} g_1(\alpha_s \widehat{L})\right), \tag{3.18}$$

where the quantity $-\frac{d}{d\widehat{L}}(\widehat{L}g_1(\alpha_s\widehat{L}))$ is referred to in some contexts as $R'(\alpha_s\widehat{L})$. Rescaling the argument of the logarithm also entails changes to the fixed-order coefficients both in the modified and unmodified cases:

$$\begin{aligned}
G_{12} \to \widehat{G}_{12} &= G_{12} \\
G_{11} \to \widehat{G}_{11} &= G_{11} + 2G_{12}\ln x_L \\
G_{23} \to \widehat{G}_{23} &= G_{23} \\
G_{22} \to \widehat{G}_{22} &= G_{22} + 3G_{23}\ln x_L \\
G_{21} \to \widehat{G}_{21} &= G_{21} + 2G_{22}\ln x_L + 3G_{23}\ln^2 x_L \\
C_1 \to \widehat{C}_1 &= C_1 + G_{11}\ln x_L + G_{12}\ln^2 x_L \\
C_2 \to \widehat{C}_2 &= C_2 + (C_1G_{11} + G_{21})\ln x_L + (C_1G_{12} + G_{22} + \tfrac{1}{2}G_{11}^2)\ln^2 x_L + \\
&\quad + (G_{23} + G_{12}G_{11})\ln^3 x_L + \tfrac{1}{2}G_{12}^2\ln^4 x_L\,.
\end{aligned} \tag{3.19}$$

Transformations of the expressions under x_μ and x_L variations are commutative and can therefore be carried out in any order. In the case of the modified R matching scheme, factors of the type $[1 - (\frac{y}{y_{\max}})^p]$ are to be applied to $\widehat{G}_{11}$ and $\widehat{G}_{21}$ (eq. 3.13) after the x_L variation.

3.3 Further estimates

Direct estimates of higher-orders. It is to be noted that for the thrust and heavy jet mass, investigations have been carried out of potential sources of higher order terms (NNLL, etc.) in the resummation, in particular those associated with the running of the coupling, using the dressed-gluon exponentiation model [23]. These estimated higher orders have a rather large effect on fits for α_s, somewhat larger than the uncertainties which are deduced in section 4. Given that these are strictly speaking only model calculations and that they exist for only a subset of the observables studied here (the thrust, heavy jet mass and C-parameter), they are not included here in the uncertainty estimates; their existence should however be kept in mind, together with the possibility that 'standard' methods (e.g. scale variations) for estimating the size of higher-order effects may be overly optimistic.

Heavy-quark effects. At M_Z, events with primary b quarks represent about 20% of all events. The theoretical calculations assume however light quarks. It is important therefore to understand the impact of heavy quarks on the theoretical predictions. Fixed order predictions with heavy quarks have been in existence for a few years [25] and distributions with b quarks are known to differ by a few percent from light-quark distributions. Once this effect is multiplied by the fraction of b quark events it becomes of the order of a percent [26], which is small relative to the other perturbative uncertainties.

Recently the first NLL resummed calculation for jet rates in heavy-quark events was completed [27] (though it is NLL for R as opposed to $\ln R$, i.e. a lesser accuracy than that used throughout this paper). Physically there are two effects at play. Firstly there is the 'dead cone' (the suppression of collinear emissions with an angle smaller than m_b/Q) which implies a modification of the double-logarithmic structure for y_3 below a critical value, y_{3c}, of order m_b^2/Q^2:

$$G_{12} \ln^2 \frac{1}{y_3} \to G_{12} \left(\ln^2 \frac{1}{y_3} - \ln^2 \frac{y_{3c}}{y_3} \right) \quad (y_3 \lesssim y_{3c}) \,. \tag{3.20}$$

Secondly higher order terms are modified because the number of active flavours (e.g. in β_0) decreases by one for the parts of the momentum integral with transverse momenta less than m_b (corresponding also to $y_3 < y_{3c}$). The authors of [27] quote effects for jet rates of the order of a 3–4% for $y_{\text{cut}} = 0.004$ with $m_b = 5\,\text{GeV}$ and $Q = M_Z$.

Currently no calculations exist for other observables. However the same physical arguments allow one to make the statement that the dead cone will lead to a modification of the double logarithms analogous to that of (3.20), below a critical value $y_c \sim m_b^n/Q^n$, with $n = 1$ for the broadenings and $n = 2$ for the thrust and C-parameter (the heavy jet mass is more complicated because of the direct b-quark mass contribution). In addition, for the thrust, jet-mass and C-parameter, in the range $m_b/Q \lesssim y \lesssim m_b^2/Q^2$, there is a mixture in the resummation of contributions with 4 and 5 active flavours.

NNL calculations. One source of future improvement in the theoretical accuracy is expected to come from calculations of higher order contributions. Considerable progress has been achieved in calculating two-loop amplitudes for the process $e^+e^- \to q\bar{q}g$ [28].

Subtraction methods at NNLO to cancel infrared and collinear divergences between the two-loop, one-loop and tree-level contributions are currently being developed (see for example [29]). It will then be necessary to combine the various elements in the form of a fixed-order Monte Carlo program (analogous to EVENT2 [22]), which can be used to calculate the $\mathcal{O}(\alpha_s^3)$ contribution to the event-shape distributions. This is expected to reduce the scale dependence (see for example [30]), especially in the three-jet region. In the two-jet region, the gain from the NNLO calculations could be more modest, because much of the α_s^3 contribution is already embodied in the NLL resummation. Improved accuracy over the full phase-space may therefore also require a NNLL resummed calculation. Progress on such calculations is also being made, though full results have so far been obtained only for observables that are somewhat simpler than event shapes, such as the Higgs p_t distribution at hadron colliders [31].

4. Estimating theoretical uncertainties

For the purpose of α_s measurements it is necessary to adopt a nominal theoretical prediction, which is to be used to determine the central value of α_s, as well as a set of variations for estimating the uncertainty on α_s.

For the matching scheme the use of modified Log(R) matching is advocated, since it has proven more stable than the modified R matching scheme, which will be used as the 'alternative' theory for uncertainty estimates.

The default value of $y_{\max}$ is the maximal possible value for any number of partons (as obtained from theoretical arguments and parton-shower simulations, table 2), while the lower limit $y'_{\max}$ is used as an extreme alternative estimate.

The options for the modification degree p are less clearly delimited — properties of certain fixed-order calculations [10, 11, 13] suggest that p should be ≥ 1. The simplest case $p = 1$ is recommended for the nominal configuration. The effect of the value of p on the extracted value of α_s is studied by fitting predictions with α_s as free parameter and $p \neq 1$ to the reference theory with $p = 1$, using weights proportional to the differential cross section. The change in α_s is depicted in figure 3. In the limit of large p the prediction turns into the disfavoured unmodified matching scheme. In general the largest difference in α_s is observed around $p = 2$, which is suggested for systematic purposes.

For the renormalisation scale, in a fixed order framework $\mu^2 = Q^2$ is the simplest, hence natural choice for the invariant scale of the process. So in order to enable straightforward comparison with existing measurements the conventional $x_\mu = 1$ is recommended, together with the standard variation range, $1/2 < x_\mu < 2$. The renormalisation scale is kept the same in the fixed order and resummation parts of the calculation — though not strictly required this is also conventional, and varying x_μ separately in the two parts of the calculation would complicate the formalism somewhat.

A novel type of systematic study is proposed for the proper resummation part of the theoretical prediction. The arbitrariness of the logarithmic terms to be resummed to all orders is formalised through the variable rescaling factor x_L. In analogy with the situation

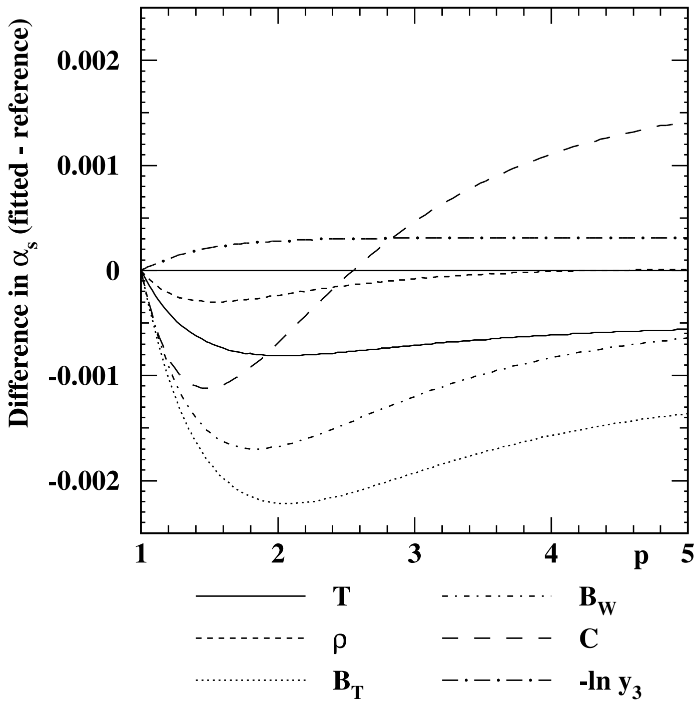

Figure 3: The change in extracted α_s as a function of the degree of modification p for several observables. As reference theory the modified Log(R) matching scheme is taken with $p = 1$. Predictions with different p are fit to the reference with α_s as free parameter.

for renormalisation scale dependence, if a resummation to all orders of logarithmic accuracy (LL, NLL, NNLL, ...) was complete then the predictions would be independent of the choice of x_L. But at any truncated order (e.g. NLL) there is a residual x_L dependence, which like the x_μ dependence, can be used to gauge the expected order of magnitude of missing higher order contributions. As in the case of the x_μ scale dependence, the range of scales can not be derived from first principles. One of the most critical elements in the measurement of α_s and estimation of the associated uncertainties is the choice of a default value and range of variation for x_L. All existing e^+e^- calculations implicitly use $x_L = 1$ and this convention has always been assumed for measurements of α_s. It is possible to argue for this as the most sensible default choice on the following grounds. In the resummation procedure, one evaluates integrals over the rapidities η and transverse momenta k_T of gluons. With the values of y_0 given after eq. (3.5), one can show that the value of the observable in the presence of a single soft and collinear gluon emission is $y \simeq y_0(k_T/Q)^a \cdot \exp(-b\eta)$, where a and b are integers. Accordingly the logarithm that is resummed, $L \equiv \ln y_0/(x_L y)$, can be rewritten $a \ln Q/k_t + b\eta - \ln x_L$. It then appears quite natural to choose the convention $x_L = 1$, since L reduces to the combination of the physical logarithms, $a \ln Q/k_t + b\eta$, without any extra constant piece.

While there exists a simple motivation for the choice of a central value of $x_L = 1$, implicitly embodied in current standard practice, the choice of the range of x_L is far more subjective and has never been considered so far. An ad hoc prescription would be to vary x_L in the same canonical range as x_μ. The effect of a given value of x_L on the distribution must be studied thoroughly, however, the objective being to find an estimate of missing higher orders. A reasonable range for x_L variations should not over-estimate the theoretical uncertainty, but complement the other investigations. Even if a strict range setting is impossible, a sensible proposal will be elaborated on the basis of various tests. This issue is studied in detail in the next subsection.

Once all these different sources of uncertainty have been examined, it is necessary to combine them, bearing in mind that there is only partial complementarity between them. This is achieved with the uncertainty band method, which is discussed in section 4.2.

4.1 Setting a range for x_L

The determination of range of variation for x_L is quite critical, because its effect is rather large. One approach is to try and find some theoretical motivation for a range, which leads to a number of possibilities:

- The observation that many of the theoretical calculation involve an inverse Mellin transform that leads naturally to logarithms of e^{γ_E}/y, suggesting a range $|\ln x_L| < \gamma_E$, where $\gamma_E \simeq .57721566$. This leads to $0.56 \le x_L \le 1.78$.
- Certain values of x_L lead to some of the subleading fixed-order expansion coefficients being zero; for example $\ln x_L = 3/4$ (twice this for $-\ln y_3$) gives $\overline{G}_{11} = 0$, suggesting $|\ln x_L| < 3/4$, i.e. $0.47 \le x_L \le 2.12$ (double for $-\ln y_3$). The appearance of a doubled range for $-\log y_3$ is natural also with the observation that for a single emission, the two-jet resolution parameter is the square of the jet broadening.
- If instead $\overline{G}_{21}$ is wanted to be zero then a quadratic equation has to be solved for $\ln x_L$, giving the results shown in table 3. Taking the solution closer to zero as more natural suggests an average range of about $|\ln x_L| \lesssim 0.6$, i.e. $0.54 \le x_L \le 1.86$.

Observable	$(\ln x_L)_-$	$(\ln x_L)_+$
T	-1.98	0.36
C	-2.39	0.76
B_T	-2.00	0.48
B_W	-1.15	0.78
$-\ln y_3$	—	—
ρ	-1.60	0.73

Table 3: Values of $\ln x_L$ which give $\overline{G}_{21} = 0$. The results typically have an error of about ± 0.05 because G_{21} is known only from fits to fixed-order Monte Carlo results. In the case of $-\ln y_3$ the solutions are complex.

Another approach consists of a comparison of the $\mathcal{O}(\alpha_s^2)$ calculation with the expansion to second order of the resummed NLL prediction. The latter is obtained by expanding eq. (3.7), keeping only terms up to $\mathcal{O}(\alpha_s^2)$. The difference between these two expression is sensitive to asymptotic terms present in the exact $\mathcal{O}(\alpha_s^2)$ calculation but absent in the NLL expansion. This Ansatz conserves the information of the differential distribution, it can be expected that in general the uncertainties are not constant across the spectra. The difference $\Delta(y)$ between the NLL expansion and the exact $\mathcal{O}(\alpha_s^2)$ calculation is determined for a central value of $\alpha_s = 0.12$. Then a theoretical variation is constructed by adding (resp. subtracting) $\Delta(y)$ to the reference prediction (i.e. using the modified Log(R) matching scheme with $x_L = 1$). Finally the reference theory

Observable	fit range 1 (nominal)	fit range 2 (2-jet)	fit range 3 (3-jet)
T	$0.70 - 0.97$	$0.87 - 0.97$	$0.70 - 0.83$
$-\ln y_3$	$2.6 - 7.2$	$5.0 - 7.2$	$2.6 - 5.0$
ρ	$0.03 - 0.25$	$0.03 - 0.12$	$0.14 - 0.25$
B_W	$0.04 - 0.20$	$0.04 - 0.12$	$0.12 - 0.20$
C	$0.08 - 0.70$	$0.08 - 0.30$	$0.38 - 0.70$
B_T	$0.05 - 0.28$	$0.05 - 0.14$	$0.15 - 0.28$

Table 4: Fit ranges used for the determination of upper and lower bounds of x_L.

Observable	x_L nominal range	x_L 2-jet range	x_L 3-jet range
T	$0.55 - 1.89$	$0.61 - 1.67$	$0.49 - 8.1$
$-\ln y_3$	$0.28 - 2.6$	$0.29 - 1.71$	$0.25 - 2.86$
ρ	$0.48 - 2.17$	$0.59 - 1.69$	$0.27 - 4.9$
B_W	$0.36 - 3.10$	$0.38 - 2.70$	$0.33 - 5.0$
C	$0.36 - 4.40$	$0.38 - 3.78$	$0.35 - 14.2$
B_T	$0.50 - 2.47$	$0.57 - 1.99$	$0.47 - 7.1$

Table 5: Ranges of x_L obtained with fits to the difference between the fixed order $\mathcal{O}(\alpha_s^2)$ calculation and the second order expansion of the NLL prediction, for three different fit ranges.

is used with variable x_L as free parameter to fit the variation. In practice, three different fit ranges, given in table 4, are used to test the stability of the procedure. The first range (nominal) covers experimental fit ranges for α_s, the second range (2-jet) is restricted to the semi-inclusive region and the third range (3-jet) comprises multi-jet production.

For the fitting procedure statistical weights scaling with the square root of the distribution value are applied. The resulting limits on x_L are given in table 5. It turns out that they strongly depend upon the range of the fit: a variation of x_L leads to a change in shape which is very large below the peak region in the two-jet limit. The effect is minimal around the peak and then increases continuously towards $y_{\max}$. The shape of $\Delta(y)$ is similar, but its slope is much steeper. This is reflected in the dependence of the results on the fit range. The resummation technique and the evaluation of $\Delta(y)$ are generally considered to be applicable in the semi-inclusive region, substantiating results obtained with the two-jet fit range. As a cross-check the same procedure is applied to the case of x_μ. In average and for the two-jet fit range a span for x_μ from 0.4 to 2.9 is found, in reasonable agreement, although slightly over-estimating the canonical range from 0.5 to 2.

The comparison with the x_μ variation can be investigated by determining x_L values such that on average, for a given set of observables (and fit ranges), the impact of the x_L variation on a fit of α_s is the same as that of the conventional x_μ variation. While at first sight this may seem to make the x_L variation procedure redundant, it should really be considered as a method for setting a conventional variation range. Different observables may then have sensitivities to the common x_L range that may be (and in practice often are) quite different. Furthermore, the y-shape of the x_L and x_μ variation will be different even if their average effect on a fit of α_s is the same, because they probe different subsets of possible higher-order corrections.

Observable	x_L nominal range	x_L 2-jet range	x_L 3-jet range
T	$0.56 - 1.77$	$0.55 - 1.78$	$0.71 - 1.55$
$-\ln y_3$	$0.48 - 2.23$	$0.27 - 2.64$	$0.59 - 2.17$
ρ	$0.58 - 1.82$	$0.56 - 1.86$	$0.82 - 1.38$
B_W	$0.67 - 1.51$	$0.63 - 1.56$	$0.79 - 1.35$
C	$0.61 - 1.71$	$0.57 - 1.81$	$0.65 - 1.54$
B_T	$0.67 - 1.53$	$0.65 - 1.54$	$0.71 - 1.46$

Table 6: Bounds of x_L obtained with a fit to the theoretical prediction with $x_\mu = 0.5$ resp. $x_\mu = 2.0$.

The procedure of this method is as follows: two predictions are calculated with the modified Log(R) scheme, $\alpha_s = 0.12$ and $x_L = 1$, one with $x_\mu = 0.5$, the other with $x_\mu = 2$. Each of them are then fitted with the same theory but $x_\mu = 1$ and x_L being the free parameter. The results are given in table 6.

Having considered this variety of criteria for choosing the x_L range, it is proposed to set a convention for the x_L range of $2/3 < x_L < 3/2$ (equivalently $|\ln x_L| \lesssim 0.405$), which gives an average uncertainty on α_s which is similar in magnitude to that from x_μ variation. This is a slightly narrower range than comes out from the purely theoretical arguments and from some of the other tests. For the purpose of a more conservative estimate of the uncertainty, or if one wishes to consider the uncertainty on the uncertainty, it is suggested to examine also a wider range $|\ln x_L| < 0.6$. Both ranges will be used for the numerical estimates in the next section.

4.2 Uncertainty band method

The new method to assess the theoretical systematic uncertainty for the measurement of α_s, called hereafter uncertainty band method, is composed of two main building blocks:

1. A nominal reference theory, the modified Log(R) matching scheme, used experimentally to determine the value of α_s.
2. A collection of theoretical uncertainties (variations of the theory) of the event-shape distributions, used to derive the perturbative uncertainty of α_s.

The following variations of the theoretical predictions for the distributions are taken into account:

- the renormalisation scale x_μ is varied between 0.5 and 2.0,
- the logarithmic rescaling factor x_L varied in between 2/3 and 3/2 (for $-\log(y_3)$ an equivalent effect is obtained with squared endpoints, *i.e.* a variation from 4/9 to 9/4),
- the modified Log(R) matching scheme is replaced by the modified R matching scheme,
- the nominal value of the kinematic constraint $y_{\max}$ is replaced by the lower limit $y'_{\max}$ and

- the first degree modification of the modified Log(R) matching scheme ($p = 1$) is replaced by a second degree modification ($p = 2$).

The uncertainty band method gives a direct relation between the uncertainty of α_s and the uncertainty of the theoretical prediction. Two pieces of information are required to calculate the systematic uncertainty: the measured value of the coupling constant, α_s^0, and the fit range used for its extraction. With these elements in hand, the uncertainty can be computed without re-fitting the data.

The method proceeds in three steps. First the reference perturbative prediction is calculated for the distribution in question using a given value for the strong coupling constant α_s^0. Then all variants of the theory mentioned above are calculated with the same value of α_s^0. In each bin of the distribution, the largest upward and downward differences with respect to the reference theory are collected. Hence the uncertainty is set by the extreme values of the theoretical variants. Variants which lead to similar but smaller effects are not double-counted. The largest differences define an uncertainty band around the reference theory.

In the last step, the reference theory is used again, but with variable α_s. In the spirit of this method, all valid theoretical predictions must lie within the uncertainty band for the fit range under consideration. Starting from the nominal α_s^0, scans of α_s are performed and the validity of resulting predictions is checked in each bin of the distribution. The largest and smallest allowed values of α_s fulfilling the condition are used to finally set the perturbative systematic error. The method is illustrated for all variables in figures 4–9, with an input value of $\alpha_s^0 = 0.12$. It might be argued that the condition for valid predictions lying strictly inside the uncertainty band is too tight, because the uncertainty is basically set by one single bin, which value is subject to statistical fluctuation of the numerically computed coefficient functions. An alternative operating mode of the uncertainty band method consists of a fit of the reference prediction to the uncertainty band envelope with α_s as free parameter. In this case weights have to be assigned to the bins inside the fit range. A convenient choice are statistical weights scaling with the square root of the distribution.

As can be seen in figures 4–9, the total theoretical uncertainty, i.e. the uncertainty band, varies drastically across the distributions. The uncertainties are large, of the order of 30%, at both ends of the spectra and reach a minimum of a few percent in the peak region. In the range of experimental fits for α_s the uncertainty of the distribution is between 5% and 10%. This turns into an uncertainty for α_s between 3% and 6%. There is also a considerable spread among the observables, the uncertainties for the total jet broadening are in the central part twice as large as for $-\ln y_3$.

A closer look at the individual components of the theoretical error reveals two major contributions: the variation of the renormalisation scale and of the x_L-scale. In the semi-inclusive region the x_μ variation generates the dominant uncertainty while in the three-jet region it is the variation of x_L. These two effects are clearly complementary. Going down in size of the uncertainty, the degree of modification as probed by the difference between $p = 1$ and $p = 2$ is important in the hard three-jet region, where this effect dominates.

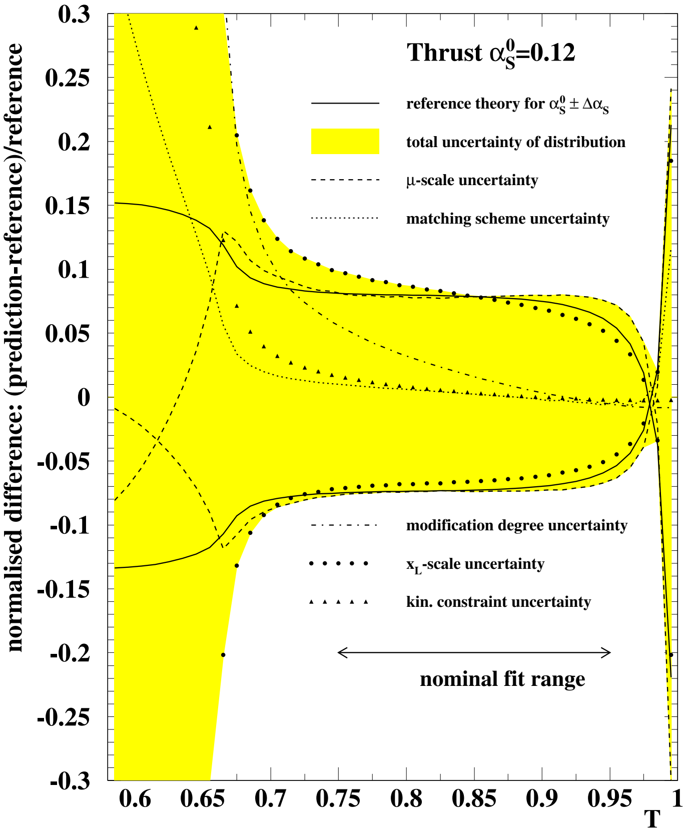

Figure 4: Theoretical uncertainties for thrust. The grey area represents the total theoretical uncertainty for the distribution. The first curve indicates the reference theory with maximum resp. minimum α_s, which determines the theoretical uncertainty $\Delta\alpha_s$ for a given measurement α_s^0. The other lines illustrate the different contributions to the theoretical uncertainty.

Both the kinematic constraint and the matching scheme uncertainty are rather small in the central part of the spectra and become somewhat larger at the multi-jet end.

The uncertainty of α_s is derived from the range of values leading to 'valid' predictions inside the uncertainty band. The resulting uncertainty depends on the fit range, which usually encloses the central part of the spectrum. The extreme, but still valid reference predictions, shown as full lines in figures 4–9, are in general determined in the central region, they touch the envelope of the uncertainty band at one point and remain inside the uncertainty band even outside the fit range.

5. Results

With the uncertainty band method as tool, all aspects of the theoretical systematic uncertainties for α_s can be studied in detail independent of a measured distribution. In table 7 results for the total uncertainty as well as for individual components are given for a representative fit range and $\alpha_s = 0.12$ as input. The total uncertainty range from 3% for $-\ln y_3$ to 6% for the total jet broadening, with an overall average of 5%. The uncertainties

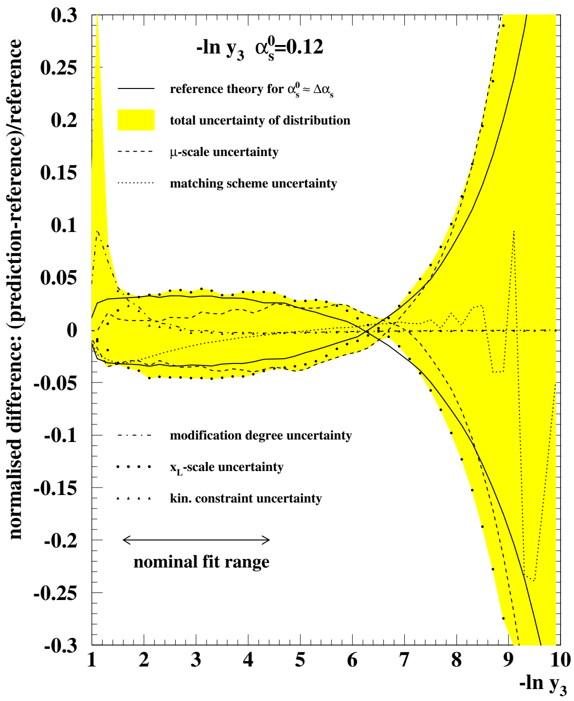

Figure 5: Theoretical uncertainties for $-\ln y_3$. The explanation is given in the caption of figure 4.

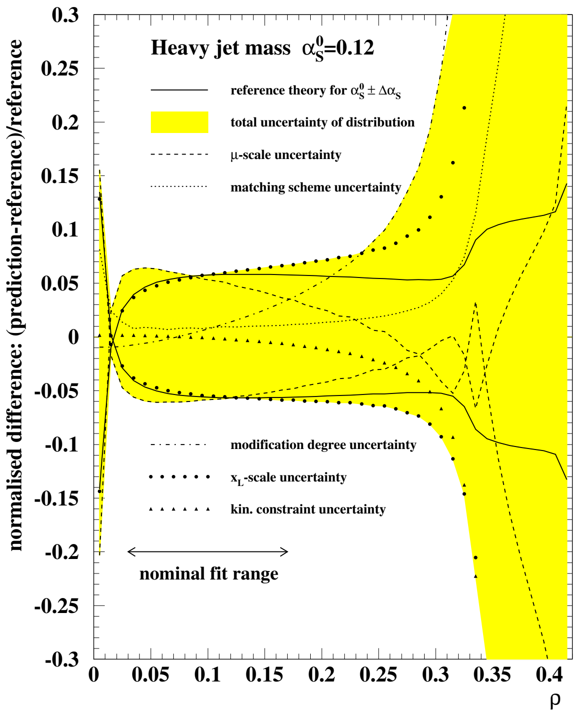

Figure 6: Theoretical uncertainties for heavy jet mass. The explanation is given in the caption of figure 4.

JHEP12(2003)007

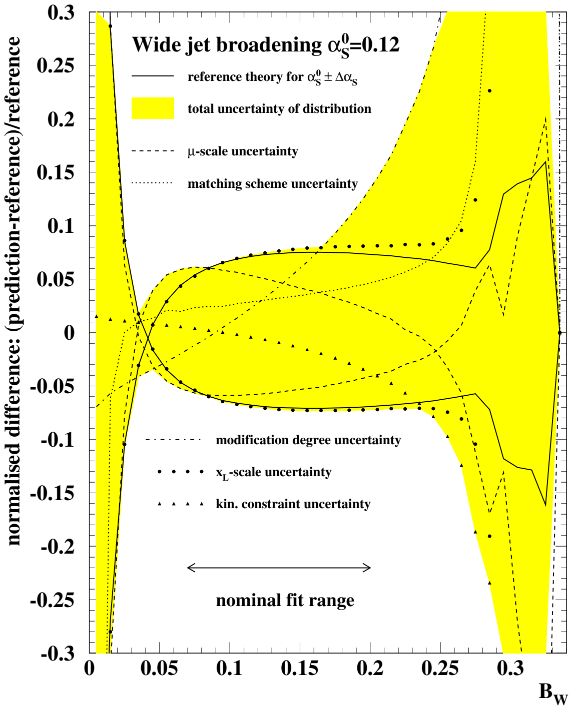

Figure 7: Theoretical uncertainties for wide jet broadening. The explanation is given in the caption of figure 4.

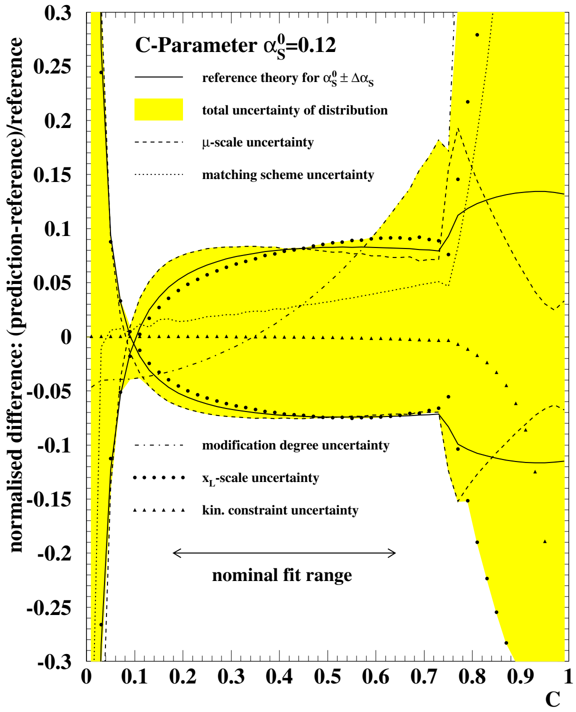

Figure 8: Theoretical uncertainties for C parameter. The explanation is given in the caption of figure 4.

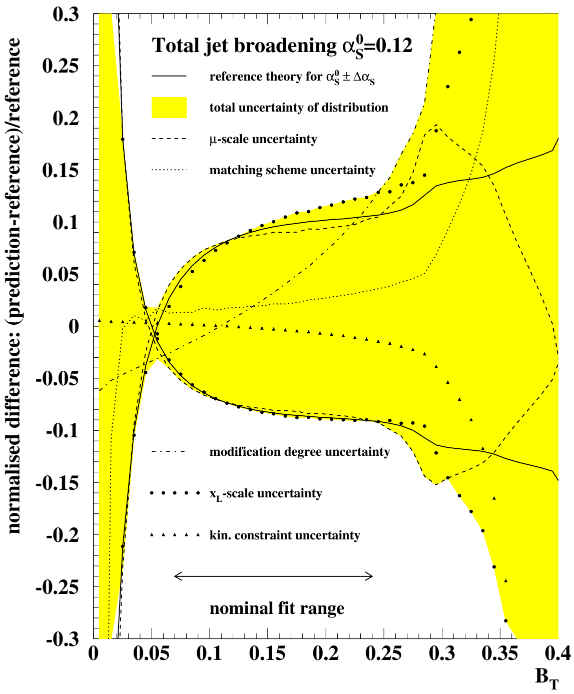

Figure 9: Theoretical uncertainties for total jet broadening. The explanation is given in the caption of figure 4.

	T	$-\ln y_3$	ρ	B_W	C	B_T
fit range	0.78-0.95	1.8-4.2	0.05-0.17	0.06-0.20	0.18-0.62	0.07-0.22
total uncertainty	+0.0057 −0.0055	+0.0028 −0.0030	+0.0044 −0.0045	+0.0055 −0.0054	+0.0058 −0.0054	+0.0068 −0.0062
x_μ uncertainty	+0.0055 −0.0055	+0.0027 −0.0008	+0.0028 −0.0039	+0.0018 −0.0033	+0.0052 −0.0053	+0.0062 −0.0059
x_L uncertainty	+0.0048 −0.0047	+0.0017 −0.0029	+0.0041 −0.0042	+0.0053 −0.0053	+0.0044 −0.0046	+0.0045 −0.0059
mod. degree uncertainty	−0.0001	+0.0002	−0.0001	−0.0004	−0.0003	+0.0003
matching scheme uncertainty	+0.0004	−0.0007	+0.0005	+0.0018	+0.0014	+0.0014
kinematic constraint uncertainty	0.0001	−0.0001	−0.0001	−0.0001	+0.0001	+0.0001
total uncertainty with $\lvert\ln x_L\rvert < 0.6$	+0.0062 −0.0059	+0.0028 −0.0032	+0.0052 −0.0052	+0.0066 −0.0066	+0.0065 −0.0061	+0.0077 −0.0073
total uncertainty with 'fit' method	+0.0062 −0.0058	+0.0032 −0.0041	+0.0052 −0.0052	+0.0061 −0.0057	+0.0066 −0.0059	+0.0074 −0.0064

Table 7: Theoretical uncertainties for $\alpha_s = 0.12$ and fit ranges given in the first row. For each variable, the total theoretical uncertainty as well as uncertainties stemming from individual sources are given. In the last two rows concern results with more conservative theory assumptions.

related to x_μ and x_L are two-sided and in general asymmetric, the other uncertainties go in a single direction. The fact that the total uncertainty is larger than any of the individual ones is a consequence of the complementary collection of uncertainties of the distributions in the uncertainty band. A clear ranking in size of the different components of the theoretical uncertainty appears for all variables: variations of x_μ and x_L are most important, followed by the matching scheme uncertainty, while the kinematic constraint and modification degree uncertainties are small and of similar size. Also given in table 7 are uncertainty estimates obtained with more conservative assumptions, namely a larger range for x_L ($|\ln x_L| < 0.6$) and a fit of the reference prediction to the uncertainty band envelope ('fit' method).

Since the uncertainty is calculated with a fixed value of α_s, the dependence of the result on the input value must be investigated. The input value, normally taken from an experimental measurement, depends on the observable and the centre-of-mass energy. For a theory defined up to $\mathcal{O}(\alpha_s^2)$, the uncertainty is formally expected to be at $\mathcal{O}(\alpha_s^3)$. The matching of fixed order and resummed calculations, however, may alter the scaling with α_s^3. The evolution of the uncertainty with α_s is shown in figure 10. In this case the symmetric uncertainty is analysed, i.e. the mean of the upward and downward uncertainty. A fit of the form $a + b\alpha_s^3$ gives a good description of the dependence of the uncertainty on α_s. The parameters a and b obtained with the fit are given in table 8 for each observable. In general a is found to be substantially smaller than $b\alpha_s^3$, confirming that to a reasonable approximation the simple α_s^3 scaling discussed above is observed.

Observable	a	b
T	$3.6\,10^{-4}$	2.99
$-\ln y_3$	$2.4\,10^{-4}$	1.51
ρ	$2.7\,10^{-4}$	2.38
B_W	$6.8\,10^{-4}$	2.71
C	$5.8\,10^{-4}$	2.88
B_T	$9.7\,10^{-4}$	3.18

Table 8: Parameterisation of the uncertainty evolution with α_s according to a form $a + b\alpha_s^3$.

The two main components of the theoretical uncertainty originate from the variations of x_μ and x_L. The size of the uncertainties depends crucially on the range of variation, nominally from 1/2 to 2 for x_μ and from 2/3 to 3/2 for x_L. The dependence on the range choice is studied by re-scaling the variation range by a factor of x_R. Hence, the re-scaled range has an upper limit of $x_{up} * x_R$ ($x_{up} = 2$ resp. $\frac{3}{2}$ for x_μ resp. x_L) and a lower limit of x_{down}/x_R ($x_{down} = \frac{1}{2}$ resp. $\frac{2}{3}$ for x_μ resp. x_L). The effect of a range variation is expected to be linear in the logarithm of the re-scaling factor x_R at least for small values of $\ln x_R$. The results are given as function of $\ln x_R$ for both the upper bound (positive error) and lower bound (negative error). The dependence of the x_μ component of the uncertainty on the range of variation is shown in figure 11. The size of uncertainty increases rapidly with the width of the range, the positive error flattens at large ranges for $-\ln y_3$, ρ and B_W. The shape of the dependence is similar for all variables. The case of the x_L component is shown in figure 12. Here the rise at small variation ranges is even steeper than for x_μ. For the variable $-\ln y_3$ the evolution is significantly flatter than for all other variables, a similar effect would have been observed with a quadratic re-scaling of the variation range.

Finally, the dependence of the uncertainty on the fit range experimentally used to extract α_s from the distribution is studied. For this purpose the uncertainty band method

JHEP12(2003)007

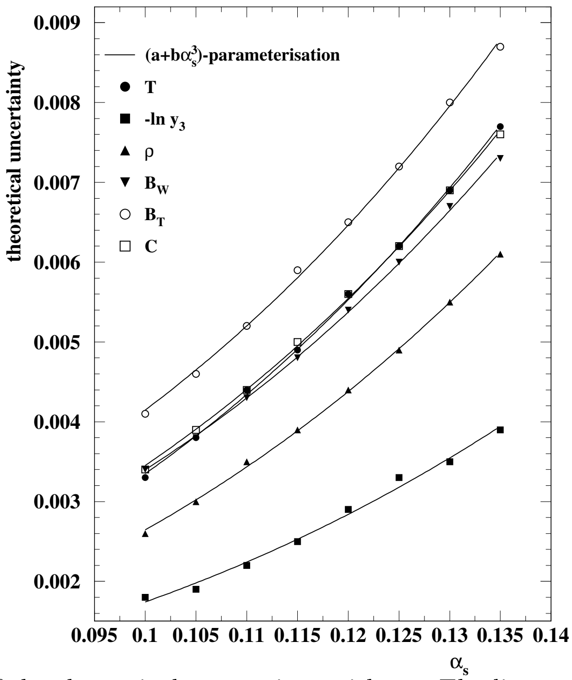

Figure 10: Evolution of the theoretical uncertainty with α_s. The lines are the result of a parameterisation scaling with α_s^3.

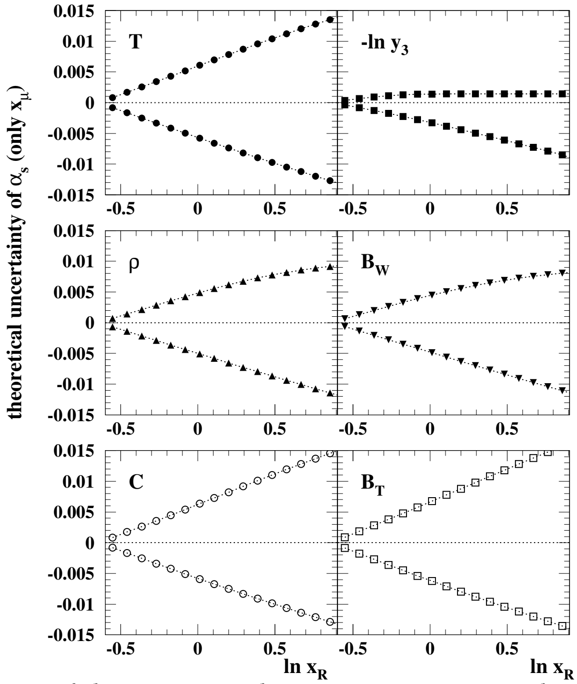

Figure 11: The dependence of the positive and negative uncertainty related to the variation of the renormalisation scale x_μ. The width of the variation range is modified such that the lower endpoint is rescaled by $1/x_R$ and the upper limit by x_R.

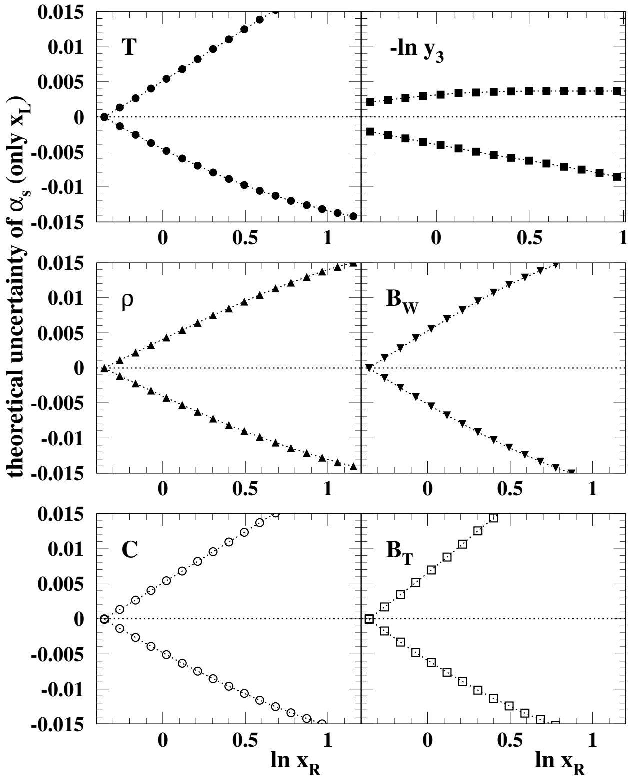

Figure 12: The dependence of the positive and negative uncertainty related to the variation of the logarithmic re-scaling factor x_L. The width of the variation range is modified such that the lower endpoint is rescaled by $1/x_R$ and the upper limit by x_R.

including all uncertainty sources is applied to each bin of the distribution, as shown in figure 13. In the central part of the distribution the uncertainty is reasonably constant and stable with respect to variations of one or two bins at each end. Approaching the peak of the distributions or the extreme three-jet region, however, induces rapidly growing uncertainties. This dependence should be kept in mind when selecting a fit range.

The theory uncertainty studies described here are all carried out on purely perturbative predictions. One could instead envisage carrying out these studies after correction to hadron-level. Whether this actually makes a difference or not depends on the details of how the hadronisation is included, for example whether as a bin-by-bin multiplicative factor, a simple shift of the distribution, or a transfer matrix. However, since hadronisation corrections will have similar effects both on the various alternate theory curves and on the reference prediction, the net impact of hadronisation is expected to be rather small and hence it is simplest and most transparent to carry out the analysis at a purely perturbative level

6. Conclusion

In this paper, a new method is presented for the assessment of theoretical uncertainties in α_s. This method evaluates the systematic uncertainty of the parameter α_s from the uncertainty of the prediction for the distributions from which it is extracted. After a

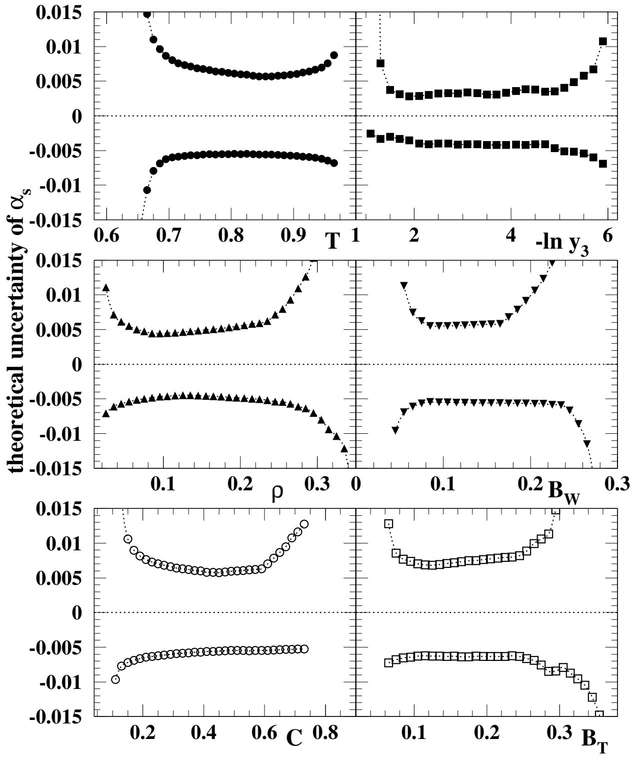

Figure 13: The dependence of the positive and negative uncertainty on the value of the observable. All components of the uncertainty are included.

comprehensive review of theoretical predictions for measurements of α_s from event-shape distributions in e^+e^- annihilation, the uncertainties of such predictions are estimated with an uncertainty band method which incorporates several variations of the theory differing in subleading terms and includes a new test for re-scaling the resummed logarithmic variables. As the uncertainty band method can compute these perturbative uncertainties of α_s independently of a measured event-shape distribution, it is especially suited for an unbiased combination of several observables or experiments.

The recommended method for computing the central result is to use the modified Log(R) matching scheme with $x_\mu = x_L = 1$, $p = 1$ and values for $y_{\max}$ given in table 2. The assessment of the perturbative uncertainty consists of a variation of the renormalisation scale x_μ from 0.5 to 2, of the logarithmic re-scaling factor x_L from $\frac{2}{3}$ to $\frac{3}{2}$, of a replacement of the modified Log(R) matching scheme by the modified R matching scheme, of the degree of modification $p = 1$ by $p = 2$ and of the kinematic constraint $y_{\max}$ by its alternative $y'_{\max}$ given in table 2. The different uncertainties should be combined with the uncertainty band method. Proposals are made for more conservative uncertainty estimates; these are a larger range for the re-scaling factor $|\ln x_L| < 0.6$ and an alternative operating mode of the uncertainty band method.

To combine several measurements from different observables or experiments the perturbative uncertainties of the individual measurements should be re-estimated with the above method using a common input value for $\alpha_s(M_Z)$ in the uncertainty band method. This input value should of course be consistent with the final result obtained iteratively.

Following these instructions even existing measurements of α_s can be equipped with an up-to-date estimation of their perturbative uncertainty and then used in a consistent combination.

Acknowledgments

We wish to thank Stefano Catani for helpful suggestions and Günther Dissertori, Einan Gardi, Klaus Hamacher and Oliver Passion for useful conversation on this subject.

References

[1] R.K. Ellis, D.A. Ross and A.E. Terrano, *The perturbative calculation of jet structure in e^+e^- annihilation*, *Nucl. Phys.* **B 178** (1981) 421.

[2] Y.L. Dokshitzer and B.R. Webber, *Calculation of power corrections to hadronic event shapes*, *Phys. Lett.* **B 352** (1995) 451 [hep-ph/9504219]; *Power corrections to event shape distributions*, *Phys. Lett.* **B 404** (1997) 321 [hep-ph/9704298];
Y.L. Dokshitzer, A. Lucenti, G. Marchesini and G.P. Salam, *On the universality of the Milan factor for 1/Q power corrections to jet shapes*, *J. High Energy Phys.* **05** (1998) 003 [hep-ph/9802381].

[3] DELPHI collaboration, P. Abreu et al., *Energy dependence of event shapes and of α_s at LEP-2*, *Phys. Lett.* **B 456** (1999) 322;
L3 collaboration, M. Acciarri et al., *QCD studies in e^+e^- annihilation from 30 GeV to 189 GeV*, *Phys. Lett.* **B 489** (2000) 65 [hep-ex/0005045];
P.A. Movilla Fernandez, S. Bethke, O. Biebel and S. Kluth, *Tests of power corrections for event shapes in e^+e^- annihilation*, *Eur. Phys. J.* **C 22** (2001) 1 [hep-ex/0105059];
DELPHI collaboration, J. Abdallah et al., *A study of the energy evolution of event shape distributions and their means with the Delphi detector at LEP*, *Eur. Phys. J.* **C 29** (2003) 285 [hep-ex/0307048];
ALEPH collaboration, A. Heister et al., *Studies of QCD at e^+e^- centre-of-mass energies between 91 and 209 GeV*, CERN-EP/2003-084.

[4] P.A. Movilla Fernandez, *α_s and power corrections from JADE*, hep-ex/0209022.

[5] LEPQCD working group, note in preparation.

[6] K.G. Chetyrkin, J.H. Kuhn and A. Kwiatkowski, *QCD corrections to the e^+e^- cross-section and the Z boson decay rate: concepts and results*, *Phys. Rept.* **277** (1996) 189;
E. Tournefier, *Extraction of α_s and constraint on the Higgs mass from electroweak fits at the Z resonance*, hep-ex/9810042.

[7] ALEPH collaboration, *A combination of preliminary electroweak measurements and constraints on the standard model*, hep-ex/0212036.

[8] K.G. Chetyrkin, B.A. Kniehl and M. Steinhauser, *Strong coupling constant with flavour thresholds at four loops in the $\overline{MS}$ scheme*, *Phys. Rev. Lett.* **79** (1997) 2184 [hep-ph/9706430].

[9] ZEUS collaboration, S. Chekanov et al., *A ZEUS next-to-leading-order QCD analysis of data on deep inelastic scattering*, *Phys. Rev.* **D 67** (2003) 012007 [hep-ex/0208023].

[10] S. Catani, G. Turnock, B.R. Webber and L. Trentadue, *Thrust distribution in e^+e^- annihilation*, *Phys. Lett.* **B 263** (1991) 491;
S. Catani, G. Turnock and B.R. Webber, *Heavy jet mass distribution in e^+e^- annihilation*, *Phys. Lett.* **B 272** (1991) 368.

[11] S. Catani, L. Trentadue, G. Turnock and B.R. Webber, *Resummation of large logarithms in e^+e^- event shape distributions*, *Nucl. Phys.* **B 407** (1993) 3.

[12] G. Dissertori and M. Schmelling, *An improved theoretical prediction for the two jet rate in e^+e^- annihilation*, *Phys. Lett.* **B 361** (1995) 167.

[13] S. Catani, G. Turnock and B.R. Webber, *Jet broadening measures in e^+e^- annihilation*, *Phys. Lett.* **B 295** (1992) 269;
Yu.L. Dokshitzer et al., *On the QCD analysis of jet broadening J. High Energy Phys.* **01** (1998) 011.

[14] S. Catani and B.R. Webber, *Resummed C-parameter distribution in e^+e^- annihilation*, *Phys. Lett.* **B 427** (1998) 377 [hep-ph/9801350].

[15] A. Banfi et al., *Semi-numerical resummation of event shapes*, *J. High Energy Phys.* **01** (2002) 018.

[16] M. Dasgupta and G.P. Salam, *Resummation of the jet broadening in DIS*, *Eur. Phys. J.* **C 24** (2002) 213 [hep-ph/0110213]; *Resummed event-shape variables in DIS*, *J. High Energy Phys.* **08** (2002) 032 [hep-ph/0208073].

[17] S. Brandt, C. Peyrou, R. Sosnowski and A. Wroblewski, *The principal axis of jets. An attempt to analyze high-energy collisions as two-body processes*, *Phys. Lett.* **A 12** (1964) 57;
E. Farhi, *A QCD test for jets*, *Phys. Rev. Lett.* **39** (1977) 1587.

[18] T. Chandramohan and L. Clavelli, *Consequences of second order QCD for jet structure in e^+e^- annihilation*, *Nucl. Phys.* **B 184** (1981) 365;
L. Clavelli and D. Wyler, *Kinematical bounds on jet variables and the heavy jet mass distribution*, *Phys. Lett.* **B 103** (1981) 383.

[19] P.E.L. Rakow and B.R. Webber, *Transverse momentum moments of hadron distributions in QCD jets*, *Nucl. Phys.* **B 191** (1981) 63.

[20] G. Parisi, *Super inclusive cross-sections*, *Phys. Lett.* **B 74** (1978) 65;
J.F. Donoghue, F.E. Low and S.-Y. Pi, *Tensor analysis of hadronic jets in quantum chromodynamics*, *Phys. Rev.* **D 20** (1979) 2759.

[21] S. Catani, Y.L. Dokshitzer, M. Olsson, G. Turnock and B.R. Webber, *New clustering algorithm for multi-jet cross-sections in e^+e^- annihilation*, *Phys. Lett.* **B 269** (1991) 432;
N. Brown and W.J. Stirling, *Jet cross-sections at leading double logarithm in e^+e^- annihilation*, *Phys. Lett.* **B 252** (1990) 657;
S. Bethke, Z. Kunszt, D.E. Soper and W.J. Stirling, *New jet cluster algorithms: next-to-leading order QCD and hadronization corrections*, *Nucl. Phys.* **B 370** (1992) 310.

[22] S. Catani and M.H. Seymour, *A general algorithm for calculating jet cross sections in NLO QCD*, *Nucl. Phys.* **B 485** (1997) 291 [hep-ph/9605323].

[23] E. Gardi and J. Rathsman, *Renormalon resummation and exponentiation of soft and collinear gluon radiation in the thrust distribution*, *Nucl. Phys.* **B 609** (2001) 123 [hep-ph/0103217]; *The thrust and heavy-jet mass distributions in the two-jet region*, *Nucl. Phys.* **B 638** (2002) 243 [hep-ph/0201019];

JHEP12(2003)007

E. Gardi and L. Magnea, *The C parameter distribution in e^+e^- annihilation*, *J. High Energy Phys.* **08** (2003) 030

[24] T. Sjöstrand et al., *High-energy physics event generation with PYTHIA 6.1*, *Comput. Phys. Commun.* **135** (2001) 238.

[25] G. Rodrigo, A. Santamaria and M.S. Bilenky, *Do the quark masses run? Extracting $m_b(m_Z)$ from LEP data*, *Phys. Rev. Lett.* **79** (1997) 193 [hep-ph/9703358];
P. Nason and C. Oleari, *Next-to-leading-order corrections to the production of heavy-flavour jets in e^+e^- collisions*, *Nucl. Phys.* **B 521** (1998) 237 [hep-ph/9709360];
A. Brandenburg and P. Uwer, *Next-to-leading order QCD corrections and massive quarks in $e^+e^- \to 3$ Jets*, *Nucl. Phys.* **B 515** (1998) 279 [hep-ph/9708350].

[26] ALEPH collaboration, R. Barate et al., *A measurement of the b-quark mass from hadronic Z decays*, *Eur. Phys. J.* **C 18** (2000) 1 [hep-ex/0008013].

[27] F. Krauss and G. Rodrigo, *Resummed jet rates for e^+e^- annihilation into massive quarks*, *Phys. Lett.* **B 576** (2003) 135 [hep-ph/0303038].

[28] L.W. Garland, T. Gehrmann, E.W.N. Glover, A. Koukoutsakis and E. Remiddi, *Two-loop QCD helicity amplitudes for $e^+e^- \to 3$ Jets*, *Nucl. Phys.* **B 642** (2002) 227 [hep-ph/0206067];
S. Moch, P. Uwer and S. Weinzierl, *Two-loop amplitudes for $e^+e^- \to q\bar{q}g$: The n_f-contribution*, *Acta Phys. Polon.* **B33** (2002) 2921 [hep-ph/0207167].

[29] S. Weinzierl, *Subtraction terms at NNLO*, *J. High Energy Phys.* **03** (2003) 062 [hep-ph/0302180]; *Subtraction terms for one-loop amplitudes with one unresolved parton*, *J. High Energy Phys.* **07** (2003) 052 [hep-ph/0306248].

[30] E.W.N. Glover, *Progress in NNLO calculations for scattering processes*, *Nucl. Phys.* **116** *(Proc. Suppl.)* (2003) 3 [hep-ph/0211412].

[31] G. Bozzi, S. Catani, D. de Florian and M. Grazzini, *The q_T spectrum of the Higgs boson at the LHC in QCD perturbation theory*, *Phys. Lett.* **B 564** (2003) 65 [hep-ph/0302104].